Acta Oceanol. Sin., 2022, Vol. 41, No. 8, P. 1–4
https://doi.org/10.1007/s13131-022-2056-7
http://www.aosocean.com
E-mail: ocean2@hyxb.org.cn

Cover Story

Oceanic internal waves generated by the Tongan volcano eruption

Xudong Zhang[1, 2], Xiaofeng Li[1, 2*]

[1] Key Laboratory of Ocean Circulation and Waves, Institute of Oceanology, Chinese Academy of Sciences, Qingdao 266071, China

[2] Center for Ocean Mega-Science, Chinese Academy of Sciences, Qingdao 266071, China

Received 8 July 2022; accepted 26 July 2022

Internal waves (IW) are widely distributed at the marginal seas or continental shelves (Liu et al., 2013; Zhao and Alford, 2006; Zheng et al., 2007). They have an amplitude of up to hundreds of meters and wave crests of several hundreds of kilometers, and affect ocean environments significantly (Wyatt et al., 2019; Zhang et al., 2022). Satellite images have played an essential role in studying IWs owing to their global-scale observation ability and multi-band sensors in orbit (Alpers, 1985; Apel et al., 1976; Lindsey et al., 2018; Zheng et al., 2001). IW generations are generally reported closely related to wind, tides, topography, and currents (Li et al., 2008; Whalen et al., 2020). Large-amplitude long-wave-crest IW is frequently generated by tide-topography interactions, lee wave mechanism, resonant mechanism, or internal tide steeping in the marginal seas (Xie et al., 2022). Small-scale IW is generated by plume mechanisms or other small-scale disturbances in coastal ocean areas (Alford et al., 2015; Jackson et al., 2012). However, IWs are rarely observed in open ocean areas because of the strong dispersion effect in the deep ocean. Here we report the first observation of IWs generated by a volcano, the Tongan volcano, eruption in the southwest of the Pacific Ocean on January 15, 2022.

Tongan volcano lies on the Pacific Plate and the Indo-Australian Plate boundary. The plate collision results in a chain of volcanoes. On January 15, 2022, the Hunga Tonga–Hunga Ha'apai, an underwater volcano (20.57°S, 175.38°W), erupted explosively and lasted 11 h. The eruption released massive energy into the ocean and triggered a tsunami, which attacked islands around Tonga. The Japanese Himawari-8 geostationary satellite images have captured the eruption sending ashes into the sky and causing atmospheric shock waves to ripple globally. An example is shown in Fig. 1a. The Himawari-8 image was downloaded from the Worldview at https://worldview.earthdata.nasa.gov/.

The European Space Agency's Sentinel-1 synthetic aperture radar (SAR) image was acquired 13 h after the initial eruption. The SAR image (Fig. 1b) shows IWs in the northern area of the volcano eruption location. SAR can observe IW because it modulates the surface gravity capillary waves and manifests as bright-dark bands on SAR images (Alpers, 1985). The Sentinel-1 SAR data were provided by European Space Agency and are available at https://scihub.copernicus.eu/dhus/#/home. Clear IW packets propagating in different directions are observed. The length of the IW crests ranges from less than 20 km to 67 km. The north propagating IWs are separated by Tofua Island, forming IW patterns similar to the IWs in the Dongsha Atoll of the South China Sea. The cross-interactions patterns imply that these IWs may not generate at a single source. Figure 2 shows the synergy observation of IWs using the Moderate-resolution Imaging Spectroradiometer (MODIS) and Sentinel-1 images with a time difference of about 5 h. The propagation speed of IWs is about 0.95 m/s. We have taken the profiles along the black line on the Sentinel-1 SAR image, as shown in Fig. 2. The characteristic wavelength of IWs ranges from 860.9 m to 1 530.4 m, which is the typical value of IWs. The length of the leading IW wave crest is 67 km.

We examined two Sentinel-1 SAR images (Figs 3a, b) acquired before (January 3) and after (January 27) the volcano eruption but did not observe IWs in this area. IW generation requires two necessary conditions: stratification and disturbing force in the water column. Figure 4 shows the stratification profiles at the IWs observation and the volcano eruption sites. The density and buoyance frequency profiles show that this area has a uniform stratification with a mixed layer depth of 65 m.

The Tongan volcano is an underwater volcano with a depth ranging from tens to 250 m (Witze, 2022). The lower heavier seawater will blow upward to the ocean surface when the volcano erupts. According to the conversation law, the lower seawater will flow to the volcano location. When the volcano eruption finished, the seawater around the volcano had a larger density in the same depth than far-field ocean areas. Therefore, the heavier seawater will move downward and spread around, disturbing the stratification. This IW generation process is similar to the IWs generated at the lab with the gravity collapse mechanism (Du et al., 2019). The heavier seawater will collapse because of the force of gravity and create a vertical shear force. An overturning potential will cause vortex motion, and the disturbance propagates along the thermocline.

On the other hand, magma will first meet seawater when the volcano erupts. The water will transform the thermal energy of the magma into kinetic energy (Witze, 2022). The kinetic energy will mainly blow upward and spread around, amplifying the oscillations induced by the collapsed heavier seawater.

Foundation item: The Strategic Priority Research Program of the Chinese Academy of Sciences under contract No. XDB42000000; the National Natural Science Foundation of China under contract Nos U2006211 and 41906157; the CAS Program under contract No. Y9KY04101L.

*Corresponding author, E-mail: lixf@qdio.ac.cn

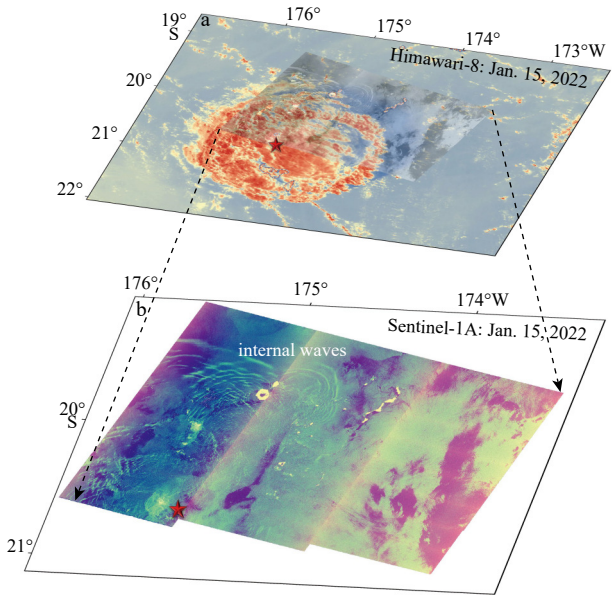

Fig. 1. Pseudo-color Himawari-8 image showing the volcano eruption (a) overlaid with Sentinel-1A image showing signatures of crescent internal waves in northern Tonga (b). The Himawari-8 image was acquired at 04:30UTC, and the Sentinel-1A synthetic aperture radar image was acquired at 17:08UTC. The red star indicates the volcano eruption location. The pseudo-color SAR image is composed with different polarization channels (VV and VH).

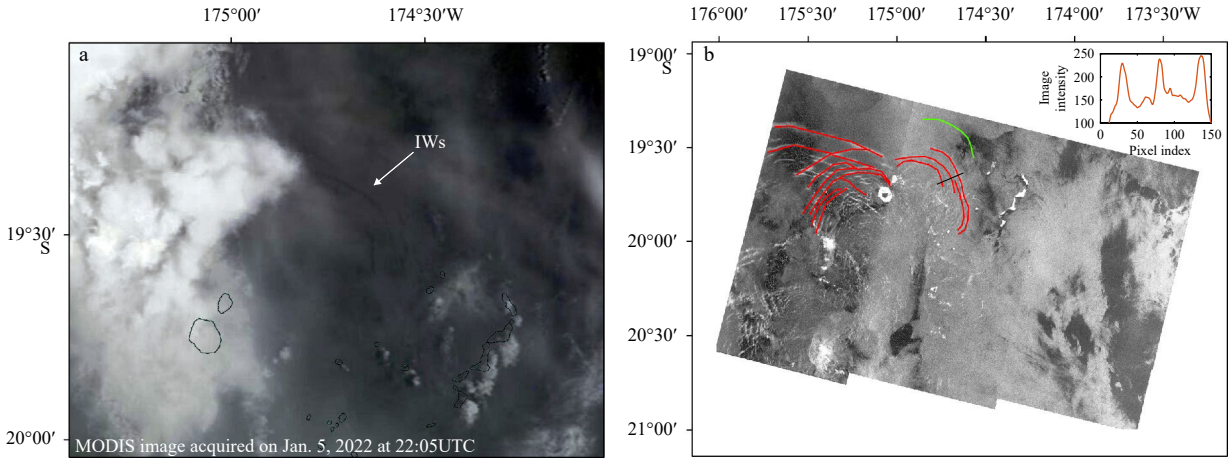

Fig. 2. Moderate-resolution Imaging Spectroradiometer (MODIS) (a) and Sentinel-1 (b) image showing signatures of internal waves in the northern Tongan. The red lines indicate the internal wave crests extracted from the Sentinel-1 image. The green line indicates the internal wave crest extracted from the MODIS image acquired 5 h later. The insert map shows the profiles taken along the black lines on the Sentinel-1 image.

From the three-dimensional underwater topography shown in Fig. 4, we can find that the energy is separated by the volcano chains, in one way propagate along the deep channel formed by collisions of Plates, and in another way leaks into the left side of the volcano chains (brown arrows in Fig. 4). When the spreading energy meets other volcanoes, the thermocline-propagating disturbance will finally evolve into IWs. Figure 4 shows that the stratification is uniform but not very strong, suggesting that disturbances, like the volcano eruption, must be extreme to produce enough energy for IW generation.

The massive power of the volcano eruption excited shock waves in the atmosphere and oceans. In previous studies, meteorological satellites have observed volcano-excited atmospheric waves (Nakashima et al., 2016). To our knowledge, this is the first time oceanic IWs are excited by a volcano eruption. The gravity collapse of seawater induced by the volcano eruption is why IW generation. The satellite images allowed the in-time observation of the volcano eruption and enriched IW generation mechanisms. No such occasions have been observed before. This fact may be attributed to three factors: fewer satellites in orbit and long revisit period of SAR images, cloud contamination of optical satellite images, and small-scale features of IWs. The bloom developing remote sensing techniques gives humans much more opportunity to observe volcano activities and their influence on the ocean.

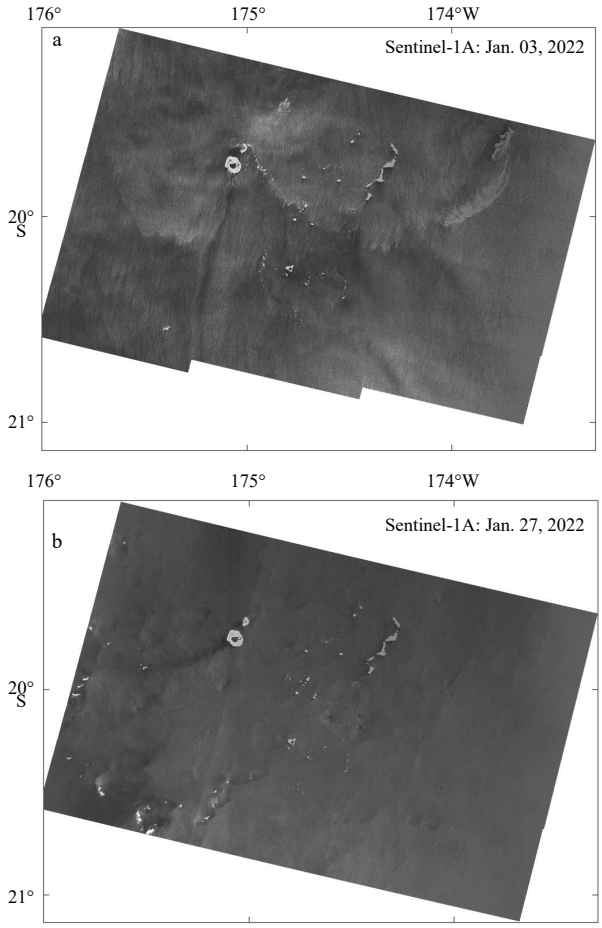

Fig. 3. Sentinel images before (a) and after (b) the Tongan volcano eruption were acquired on January 3 and January 27, 2022.

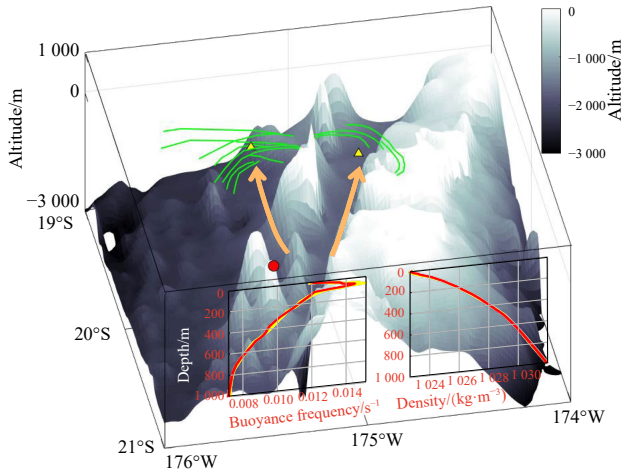

Fig. 4. Internal waves (IW) crests overlaid on the topography. The red dot indicates the location where the volcano erupted. Two yellow triangles indicate where IWs are observed and where the density information is extracted. The green lines indicate the IW crests extracted from the Sentinel-1 image. The brown arrows indicate the energy propagation path.

References

Alford M H, Peacock T, MacKinnon J A, et al. 2015. The formation and fate of internal waves in the South China Sea. Nature, 521(7550): 65–69, doi: 10.1038/nature14399

Alpers W. 1985. Theory of radar imaging of internal waves. Nature, 314(6008): 245–247, doi: 10.1038/314245a0

Apel J R, Byrne H M, Proni J R, et al. 1976. A study of oceanic internal waves using satellite imagery and ship data. Remote Sensing of

Environment, 5: 125–135, doi: 10.1016/0034-4257(76)90043-2

Du Hui, Wei Gang, Wang Shaodong, et al. 2019. Experimental study of elevation- and depression-type internal solitary waves generated by gravity collapse. Physics of Fluids, 31(10): 102104, doi: 10.1063/1.5121556

Jackson C R, da Silva J C B, Jeans G. 2012. The generation of nonlinear internal waves. Oceanography, 25(2): 108–123, doi: 10.5670/oceanog.2012.46

Li Xiaofeng, Zhao Zhongxiang, Pichel W G. 2008. Internal solitary waves in the northwestern South China Sea inferred from satellite images. Geophysical Research Letters, 35(13): L13605, doi: 10.1029/2008GL034272

Lindsey D T, Nam S, Miller S D. 2018. Tracking oceanic nonlinear internal waves in the Indonesian seas from geostationary orbit. Remote Sensing of Environment, 208: 202–209, doi: 10.1016/j.rse.2018.02.018

Liu Antony K, Su Feng-Chun, Hsu Ming-Kuang, et al. 2013. Generation and evolution of mode-two internal waves in the South China Sea. Continental Shelf Research, 59: 18–27, doi: 10.1016/j.csr.2013.02.009

Nakashima Y, Heki K, Takeo A, et al. 2016. Atmospheric resonant oscillations by the 2014 eruption of the Kelud volcano, Indonesia, observed with the ionospheric total electron contents and seismic signals. Earth and Planetary Science Letters, 434: 112–116, doi: 10.1016/j.epsl.2015.11.029

Whalen C B, de Lavergne C, Naveira Garabato A C, et al. 2020. Internal wave-driven mixing: governing processes and consequences for climate. Nature Reviews Earth & Environment, 1(11): 606–621

Witze A. 2022. Why the Tongan eruption will go down in the history of volcanology. Nature, 602(7897): 376–378, doi: 10.1038/d41586-022-00394-y

Wyatt A S J, Leichter J J, Toth L T, et al. 2019. Heat accumulation on coral reefs mitigated by internal waves. Nature Geoscience, 13(1): 28–34

Xie Huarong, Xu Qing, Zheng Quanan, et al. 2022. Assessment of theoretical approaches to derivation of internal solitary wave parameters from multi-satellite images near the Dongsha Atoll of the South China Sea. Acta Oceanologica Sinica, 41(6): 137–145, doi: 10.1007/s13131-022-2015-3

Zhang Xudong, Wang Haoyu, Wang Shuo, et al. 2022. Oceanic internal wave amplitude retrieval from satellite images based on a data-driven transfer learning model. Remote Sensing of Environment, 272: 112940, doi: 10.1016/j.rse.2022.112940

Zhao Zhongxiang, Alford M H. 2006. Source and propagation of internal solitary waves in the northeastern South China Sea. Journal of Geophysical Research: Oceans, 111(C11): C11012, doi: 10.1029/2006JC003644

Zheng Quanan, Susanto R D, Ho Chung-Ru, et al. 2007. Statistical and dynamical analyses of generation mechanisms of solitary internal waves in the northern South China Sea. Journal of Geophysical Research: Oceans, 112(C3): C03021

Zheng Quanan, Yuan Yeli, Klemas V, et al. 2001. Theoretical expression for an ocean internal soliton synthetic aperture radar image and determination of the soliton characteristic half width. Journal of Geophysical Research: Oceans, 106(C12): 31415–31423, doi: 10.1029/2000JC000726